Optics Letters

Wide-field optical coherence tomography angiography enabled by two repeated measurements of B-scans

Ruikang K. Wang,[1,*] Anqi Zhang,[1] Woo June Choi,[1] Qinqin Zhang,[1] Chieh-li Chen,[1] Andrew Miller,[2] Giovanni Gregori,[2] and Philip J. Rosenfeld[2]

[1]University of Washington, Department of Bioengineering, Seattle, Washington 98195, USA
[2]University of Miami Miller School of Medicine, Bascom Palmer Eye Institute, Miami, Florida 33136, USA
*Corresponding author: wangrk@uw.edu

Received 23 February 2016; revised 12 April 2016; accepted 15 April 2016; posted 18 April 2016 (Doc. ID 259889); published 11 May 2016

Optical coherence tomography angiography (OCTA) has increasingly become clinically important, particularly in ophthalmology. However, the field of view (FOV) for current OCTA imaging is severely limited due to A-scan rates that can be afforded by current clinical systems and, more importantly, the requirement of a repeated scanning protocol. This Letter evaluates the possibility of using only two repeated B-scans for OCTA for the purpose of an increased FOV. The effect of repeated numbers on the OCTA result is discussed through experiments on an animal model *in vivo* and evaluated using quantitative metrics for image quality. Demonstrated through *in vivo* imaging of a pathological human eye, we show that optical microangiography-based OCTA with two repeated B-scans can provide wide-field angiography up to 12 × 12 mm with clinically acceptable image quality.

OCIS codes: (110.4500) Optical coherence tomography; (170.3880) Medical and biological imaging; (170.2655) Functional monitoring and imaging.

http://dx.doi.org/10.1364/OL.41.002330

Optical coherence tomography (OCT)-based angiography (OCTA) is increasingly becoming one of the key imaging technologies in the field of biomedical imaging, particularly in ophthalmology [1–4]. Fluorescein angiography (FA) and indo-cyanine green angiography (ICGA) are the *de facto* standard in imaging vasculature within the posterior pole of the human eye. However, the need for the intravenous injection of contrasting dyes and relatively long procedure time (>10 min) make them less than ideal for routine and repeated use in patients. In contrast, OCTA is a noninvasive, cost-effective, rapid (seconds) and safe (without the need for dye injection) imaging technique, and capable of providing three-dimensional (3D) retinal vascular networks, thus having potential in the longitudinal monitoring of therapeutic treatment of eye diseases. Owing to these attributes, OCTA has been rapidly moved into the clinic for the investigation of a number of retinal diseases, such as diabetic retinopathy ([2]), macular telangiectasia ([5]), branch retinal vein occlusion ([6]), and age-related macular degeneration ([7]).

OCTA relies on particle (e.g., red blood cells) motion to contrast blood flow within a scanned tissue volume. This motion contrast requires a time series of OCT signals at one location to extract blood flow signals for OCTA reconstruction. This is achieved by repeated B-scans at one location, a strategy adopted by almost all of the current clinical OCTA systems. The greater the number of repeated B-scans used, the better the signal-to-noise ratio of the final OCTA. However, as the number of repeated B-scans increases, the FOV becomes more limited, given the constraint of current clinical OCT systems with a maximal imaging speed of 100 kHz at best. As a consequence, most published high-quality OCTA results have so far been limited to a FOV of 3 × 3 mm with $N \geqq 4$ repeated scans at one location. For example, Zhang *et al.* [5] and Kashani *et al.* [6], respectively, studied neovascular macular telangiectasia type 2 and retinal vein occlusions using a prototype swept source and spectral domain OCTA instruments (Carl Zeiss Meditec, Inc.). B-scans were repeated four times at each position and high-quality angiograms of retinal layers were presented. A recent study of choroidal neovascularization (CNV) by Miere *et al.* used the AngioVue OCTA system (Optovue, Inc.) that utilized two consecutive orthogonal volume scans with two repeated B-scans, resulting in a total of four repeated B-scans at each location [7], providing reasonable OCTA images of CNV. While these reports utilized four repeated measurements, the imaging field of view (FOV) was limited to 3 × 3 mm. This fact has more or less slowed down the clinical acceptance of OCTA when compared with FA or ICGA where the imaging FOV is typically 30 deg or greater. As a reference, a 40 deg FOV is ∼12 × 12 mm.

To achieve large FOV for OCTA imaging, we have used a so-called "montage" scanning strategy [8] in which the imaging volume is divided into $M \times M$ cubes, and each cube is imaged sequentially. The results of individual cubes were then stitched together to result in a retinal angiogram with a wide FOV of more than 50 deg. While promising, this method is

cumbersome, considering the relatively long total imaging time (>120 s). Alternatively, another solution is to use fewer repeated B-scans during scanning. However, it is currently unclear how many repeated scans would be necessary to achieve OCTA with clinically acceptable image quality. One question is whether it is feasible to obtain images with a large FOV by using fewer repeated B-scans (e.g., $N = 2$) while still being able to visualize important pathological information. The purpose of this Letter is to evaluate the effect of the number of B-scans at one location on the final *en-face* angiograms using OCT-based angiographic algorithms, and demonstrate the feasibility of using only two repeated measurements. It is expected that this Letter would provide useful guidance for the selection of repetition numbers in OCTA.

To evaluate the effect of the repetition numbers on the final OCTA results, we choose to use an ultrahigh sensitive optical microangiography (OMAG) algorithm [9,10] because it utilizes both amplitude and phase information available in OCT signals to contrast blood flow and provides better OCTA image quality compared with other algorithms [1], such as speckle variance [11], decorrelation mapping [12], and phase variance [13]. To eliminate the possible artifacts due to sample movements, it would be ideal if a living sample is stable. For this reason, we elected to image cerebral blood flow in an animal model for the purpose of this evaluation because the animal can be immobilized under anesthesia during imaging. In the experiment, one young adult mouse (strain: C57BL/6) was used, and a cranial window was prepared for easy access to the brain cortex.

To collect the datasets for evaluation, a spectral domain OCT system operating at 1300 nm wavelength was employed that had an A-scan rate of 92 kHz [14], enabling a B-frame rate of 200 Hz, with each B-scan consisting of 400 A-line scans. The system had measured axial and lateral resolution of ~6 μm in tissue. The OCTA scanning protocol was similar to that described in [14], where a total of 400 scan positions along the slow axis were obtained. At each position, the B-scan was repeated 12 times. The FOV was 2 × 2 mm (slow × fast axis). The resulting dataset was then subject to the OMAG algorithm to generate the final OCTA results by varying the repetition numbers of B-scans from 2 to 12.

Figures 1(a)–1(d) illustrate the *en face* vascular images of mouse brain vasculature for $N = 2$, 4, 8, and 12, respectively, produced by a maximum amplitude projection (MIP) of the OCTA results along a depth of ~0.5 mm below the cortical tissue surface. 0.5 mm depth was chosen because the OCT signal was not severely attenuated at this range. It is evident that the OCT angiogram becomes increasingly clearer with the increase of N from 2 to 12. Surprisingly, the result from $N = 2$ gives acceptable visible appearance of cerebral blood vessel networks, even though the experiment was conducted *in vivo*. To better visualize the differences, the region marked by the white box in Figs. 1(a)–1(d) was magnified three times in Figs. 1(e)–1(h), where the image quality difference among varied Ns can be more appreciated as judged visually by the smoothness of vessel networks and noise background of the image.

To objectively evaluate the images, we quantitatively assessed the effect of N on the OCTA results. Two metrics similar to the previous ones were employed [1]. These metrics included vessel connectivity and the image signal-to-noise ratio (SNR). To do so, a ground truth of the vessel network is required, which unfortunately is not available. To mitigate this problem, we used the vascular networks resulting from $N = 12$ [Fig. 1(d)] as a surrogate. Such treatment is reasonable because the total scanning time for $N = 12$ amounted to ~12 s, which is more than sufficient to capture all possible blood flow within the scanned tissue volume. Furthermore, the averaging operation among all the 12 repeated scans would generate a final image whose SNR approaches the true ground state. Therefore, in this evaluation, Fig. 1(d) was considered as the "ground truth" angiogram to generate the vessel area map and skeletonized blood vessel network, upon which the vessel connectivity and image SNR were calculated. The vessel area map was obtained through morphological operations as described in [15], where the original image was low pass filtered and then binarized by a local adaptive threshold within a predefined window size of 5 × 5 pixels. Figure 2(b) illustrates the vessel area map, $V(x, y)$, resulting from the original image in Fig. 2(a), $I(x, y)$. Then, all the blood vessels in the vessel area map were shrunk into one pixel width, resulting in a skeletonized vessel network as shown in Fig. 2(c), which represent the "true" vascular network, $S(x, y)$, for all the pixels. Because the relatively large vessels have higher intensity values as shown in Fig. 2(a), the arterioles and venules with sizes more than 30 μm [Fig. 2(d), $M(x, y)$] were excluded from the analysis to minimize the effect of these vessels on the assessment of the vessel connectivity and SNR. In doing so, three binary images of $V(x, y)$, $S(x, y)$, and $M(x, y)$ were generated that are used to evaluate the images $I_N(x, y)$ produced from $N = 2$ to 12.

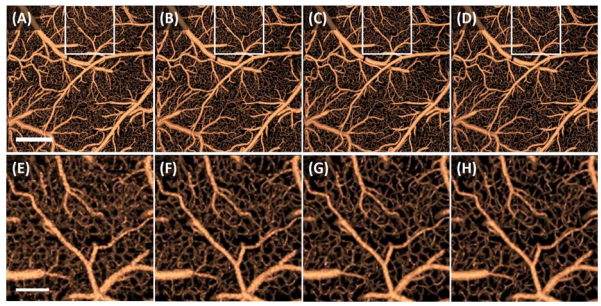

Fig. 1. OCT angiograms of mouse brain vasculature generated by varying the number of repeated B-scans: (a) $N = 2$, (b) 4, (c) 8, and (d) 12, respectively. (e)–(h) are the magnified images corresponding to the white boxes in (a)–(d), respectively. The bar = 500 μm in the upper row and 150 μm in the lower row.

The vessel connectivity was calculated as

$$\text{Connectivity} = \boldsymbol{std}\left[\boldsymbol{I_N(x,y)}|_{[\boldsymbol{V(x,y)!==M(x,y)]==1}}\right], \quad \textbf{(1)}$$

where the standard deviation of vascular intensity is evaluated, the logical operator "!==" means "not equal", and "==" denotes "equal". Hence, the smaller this value, the smoother the vessel. The image SNR was calculated as the ratio of the signal mean to the standard deviation of the background signals:

$$\text{SNR} = \frac{\text{mean}\left[I_N(x,y)|_{[V(x,y)!==M(x,y)]==1}\right]}{\text{std}\left[I_N(x,y)|_{[V(x,y)!==M(x,y)]==0}\right]}. \quad \textbf{(2)}$$

With the above definitions, the quantitative metrics were calculated for N ranging from 2 to 12. The results are illustrated in Fig. 2(e), indicating that the repetition number at $N = 4$ gives a good balance to obtain images with sufficient quality

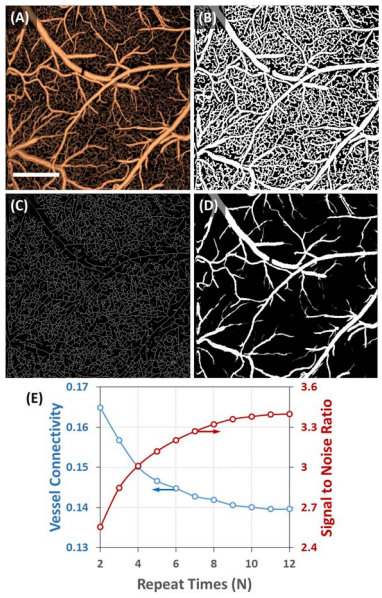

Fig. 2. Quantitative evaluation of OCT angiograms generated by varying N. (a) "Standard" image; (b) vessel area map; (c) skeletonized vascular map; and (d) larger vessel map with diameter > 30 μm, generated from (a). (e) Plot of vessel connectivity (blue) and image SNR (red) by varying N. Bar = 500 μm.

to provide both subjective and objective assessment of the results, which agrees well with the number ($N = 4$) currently used in most commercial OCTA systems. Considered individually, the vessel connectivity improves with the increase of repetition times. The rate of improvement is steepest from $N = 2$ to 4. After $N = 4$, the improvement rate slows and almost reaches a plateau at $N > 10$, indicating that a further increase of $N > 4$ would probably not provide a big advantage in improving the vessel connectivity in the OCTA images. The same conclusion is also true for SNR assessment. These objective assessments agree well with the visual assessment of the images shown in Fig. 2. However, it was noticed that at $N = 2$, the OCTA image still gives a SNR value of 2.5. According to the basic visual perception of a target in a noisy background [16], an imagery with a SNR of >2 (3 dB) would meet the visual requirement for humans to detect target features within a noisy background. Therefore, the results from just two repetitions of B-scans would still be useful for detecting vascular features from the OCTA images, although the vessel connectivity is low, and that might prevent quantitative assessment of the OCTA images for clinical diagnostic purposes. Thus, if the purpose is only for qualitative visual impressions, then we may conclude that OCTA with $N = 2$ would convey useful information to aid clinicians and physicians for a quick qualitative evaluation of the overall vascular status. This conclusion for the repetition time of $N = 2$ is clinically important for the following reasons: (1) it would translate to less time required to obtain OCTA images from patients provided that the FOV is fixed, thus increasing patient compliance for imaging; (2) on the other hand, it would provide us with an opportunity to perform wider FOV scans on the sample because for a fixed imaging duration, a greater number of A-scans for a B-scan can now be afforded. The latter is more clinically plausible, for example, in retinal imaging of DR patient where it is desirable to have wide-field scans on the retina so that the vascular information in the more peripheral regions can be visualized for the clinical examination.

Based on the above analysis, we hypothesize that with the OMAG algorithm, it would be feasible to generate a clinically acceptable retinal vasculature map when $N = 2$ for visual assessment in human subjects. To test this hypothesis, we conducted clinical imaging on a patient diagnosed with DR using a Zeiss swept source (1060 nm central wavelength) OCT angiography prototype that has an A-line scan rate of 100 kHz. Images were collected from the same patient using three scanning protocols, covering a FOV of 3 × 3 mm (FOVa), 6 × 6 mm (FOVb), and 12 × 12 mm (FOVc) centered at fovea, respectively. For the FOVa, the total number of B-scans is 1200 captured at a system frame rate of ~300 frames per second, taking 4 sec to complete. Each B-scan consisted of 300 A-lines, while $N = 4$ was used at each lateral (or transverse) position with 300 positions along the slow axis. For the FOVb, $N = 2$ was used at each of 420 lateral positions along the slow axis. Each B-scan consists of 420 A-lines. One set of volumetric scans had a total of 820 B-scans, also taking ~4 sec to complete. In the FOVc, there were 500 lateral positions along the slow axis that were sampled with $N = 2$. Within each B-scan, there were 500 A-scans, and a total of 1000 B-scans were collected for one 3D scan, taking ~5 s. Because the FOVa was collected with $N = 4$, it was straightforward to generate the OCTA result for $N = 2$ from the dataset available. The results of the three FOVs are illustrated in Figs. 3(a)–3(d), respectively.

Overall, agreement of the vascular appearance in OMAG images at the central macular region was reached among all the different scan protocols. Compared with Fig. 3(a), the vascular networks in Fig. 3(b) look similar, but with better smoothness of vessel connections (0.151 versus 0.162) and less noise background (SNR = 2.98 versus 2.52), as expected. Though produced with $N = 2$, almost all the features in Fig. 3(b) can be visualized in Figs. 3(c) and 3(d) with some exceptions, such as the vessels indicated by the thin arrows. In Fig. 3(b), the vessel pointed to by the thin arrow indicates the good connection of two vasculature networks. However, this connection is not obvious in Figs. 3(c) and 3(d). Nonetheless, the results produced by $N = 2$ with a FOV of 6 × 6 mm and 12 × 12 mm carry more pathological information, particularly in the peripheral regions away from central fovea, which can be clinically important in the assessment of DR. For this DR case, the dropout of the retinal vessel is appreciated better in the larger FOV, e.g., those areas marked by stars and thick arrows, which are not imaged in the 3 × 3 mm central macular scans. The results speak for themselves, demonstrating the feasibility of using $N = 2$ to obtain wide FOV OCT angiograms in humans. It should be noted that the quality of OCTA is affected by the spacing between adjacent A-scans. In Fig. 3(a), the spacing was 10 um, while it was 14.3 and 24 um for Figs. 3(c) and 3(d), respectively. The relatively larger spacing for wide FOVs may also contribute to a decreased image quality of final OCT angiograms, but the image quality in all these scans appears to be similar, thus demonstrating the utility of this strategy in routine clinical care.

The findings of this Letter are highly clinically significant. By demonstrating that clinically useful OCTA images can be

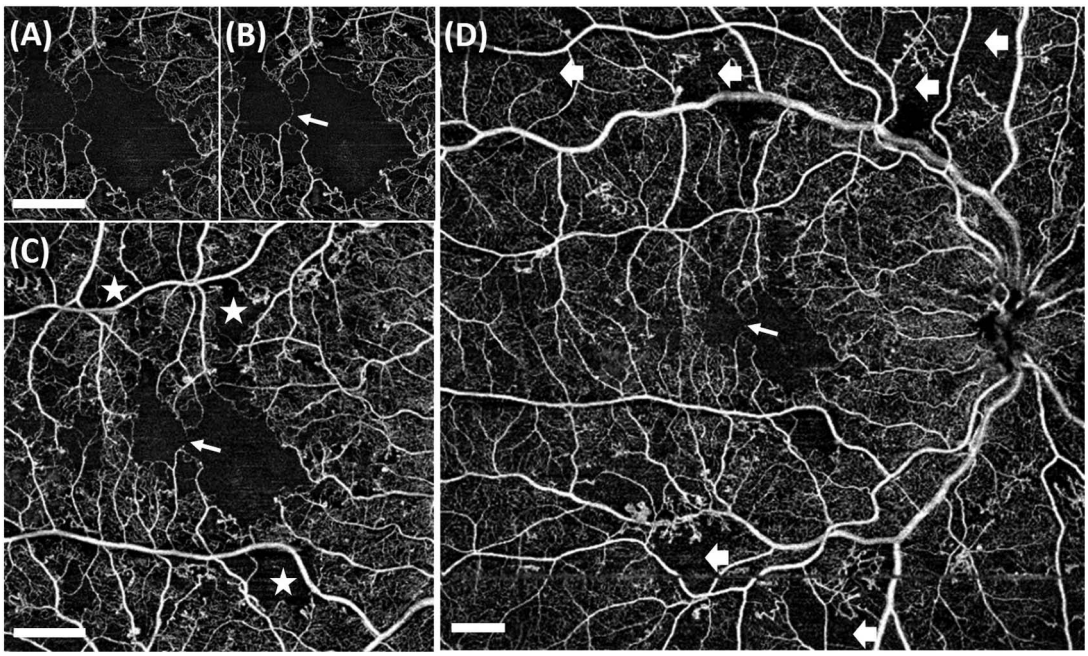

Fig. 3. OCTA images of a human subject diagnosed with diabetic retinopathy. (a) and (b) cover 3×3 mm with $N = 2$ and 4, respectively. (c) 6×6 mm with $N = 2$ and (d) 12×12 mm with $N = 2$. Bar = 1.0 mm.

obtained using OMAG and two repeated B-scan measurements, we have shown that a larger FOV of up to 12×12 mm can be achieved for the quick qualitative assessment of a diseased eye so that regions of interest can be identified for further detailed investigation. If necessary, the system can then be used to focus on a region of interest for a smaller FOV, for example 3×3 mm using four repeated B-scan measurements, to visualize the vasculature in greater detail. The quantitative analysis can then be conducted with high-quality OCTA images.

In summary, we have demonstrated that the use of $N = 2$ is feasible for OCTA to generate wide FOV imaging scans in humans. Evaluated from cerebral microcirculation imaging in an animal model, we have shown that the vascular connectivity (smoothness) and the image SNR improves with an increase of N. The image SNR was ~2.5 when $N = 2$, which provided the rationale for using an $N = 2$ in OCTA to generate visually and clinically useful angiograms from living subjects. Finally, we demonstrated the clinical usefulness of using $N = 2$ to provide wide-field FOV imaging of up to 12×12 mm in patients, thus increasing the utility of OCTA for ophthalmic imaging of human diseases.

Funding. National Heart and Lung Institute (NHLI) (R01HL093140); National Eye Institute (NEI) (R01EY024158); Carl Zeiss Meditec, Inc.

Acknowledgment. The animal procedures described in the Letter were reviewed and approved by the IACUC of University of Washington. The human imaging procedures were reviewed and approved by University of Miami Miller School of Medicine Institutional Review Board.

REFERENCES

1. A. Q. Zhang, Q. Q. Zhang, C. L. Chen, and R. K. Wang, J. Biomed. Opt. **20**, 100901 (2015).
2. Y. L. Jia, S. T. Bailey, T. S. Hwang, S. M. McClintica, S. S. Gao, M. E. Pennesi, C. J. Flaxel, A. K. Lauer, D. J. Wilson, J. Hornegger, J. G. Fujimoto, and D. Huang, Proc. Natl. Acad. Sci. USA **112**, E2395 (2015).
3. D. Y. Kim, J. Fingler, R. J. Zawadzki, S. S. Park, L. S. Morse, D. M. Schwartz, S. E. Fraser, and J. S. Werner, Proc. Natl. Acad. Sci. USA **110**, 14354 (2013).
4. I. Gorczynska, J. V. Migacz, R. J. Zawadzki, A. G. Capps, and J. S. Werner, Biomed. Opt. Express. **7**, 911 (2016).
5. Q. Zhang, R. K. Wang, C. L. Chen, A. D. Legarreta, M. K. Durbin, L. An, U. Sharma, P. F. Stetson, J. E. Legarreta, L. Roisman, G. Gregori, and P. J. Rosenfeld, Retina **35**, 2285 (2015).
6. A. H. Kashani, S. Y. Lee, A. Moshfeghi, M. K. Durbin, and C. A. Puliafito, Retina **35**, 2323 (2015).
7. A. Miere, O. Semoun, S. Cohen, A. El Ameen, M. Srour, C. Jung, H. Oubraham, G. Querques, and E. H. Souied, Retina **35**, 2275 (2015).
8. Q. Q. Zhang, Y. Huang, T. Zhang, S. Kubach, L. An, M. Laron, U. Sharma, and R. K. Wang, J. Biomed. Opt. **20**, 066008 (2015).
9. R. K. Wang, S. L. Jacques, Z. Ma, S. Hurst, S. R. Hanson, and A. Gruber, Opt. Express **15**, 4083 (2007).
10. R. K. Wang, L. An, P. Francis, and D. J. Wilson, Opt. Lett. **35**, 1467 (2010).
11. A. Mariampillai, B. A. Standish, E. H. Moriyama, M. Khurana, N. R. Munce, M. K. K. Leung, J. Jiang, A. Cable, B. C. Wilson, I. A. Vitkin, and V. X. D. Yang, Opt. Lett. **33**, 1530 (2008).
12. J. Enfield, E. Jonathan, and M. J. Leahy, Biomed. Opt. Express **2**, 1184 (2011).
13. J. Fingler, D. Schwartz, C. Yang, and S. E. Fraser, Opt. Express **15**, 12636 (2007).
14. U. Baran, Y. D. Li, and R. K. Wang, Neurophotonics **2**, 025006 (2015).
15. R. Reif, J. Qin, L. An, Z. Zhi, S. Dziennis, and R. K. Wang, Int. J. Biomed. Imaging **2012**, 509783 (2012).
16. R. G. Swensson and P. F. Judy, Percept. Psychophys. **29**, 521 (1981).